Proceedings of MICROMINI 2005
3rd International Conference on Microchannels and Minichannels
June 13-15, 2005, Toronto, Ontario, Canada

ICMM2005-75108

PRESSURE DROP OF FULLY-DEVELOPED, LAMINAR FLOW IN ROUGH MICROTUBES

M. Bahrami[1], M. M. Yovanovich[2], and J. R. Culham[3]
Microelectronics Heat Transfer Laboratory
Department of Mechanical Engineering
University of Waterloo, Waterloo, ON, Canada N2L 3G1

Abstract

The characteristics of fully-developed, laminar, pressure-driven, incompressible flow in rough circular microchannels are studied. A novel analytical model is developed that predicts the increase in pressure drop due to wall roughness in microtubes. The wall roughness is assumed to posses a Gaussian isotropic distribution. The present model is compared with experimental data, collected by other researchers and good agreement is observed.

Nomenclature

a	=	mean radius of rough microtube, m
C	=	Darcy's friction coefficient, fRe_D
D	=	microtube inside diameter, m
f	=	Darcy's friction factor, $[-]$
f^*	=	normalized friction factor, f/f_0
L	=	microtube length, m
$\dot{m}$	=	mass flow rate, kg/s
p, q	=	random variables, m
R_a	=	arithmetic average wall roughness, m
r	=	radius, m
Re_D	=	Reynolds number, $\rho\overline{u}D/\mu$
R_f	=	frictional resistance, $m^{-1}s^{-1}$
R_f^*	=	normalized frictional resistance, $R_f/R_{f,0}$
R_q	=	RMS wall roughness, m
T	=	mean fluid temperature, $^\circ C$
$\overline{u}$	=	mean fluid velocity, m/s
z	=	measured values of surface heights, m

Greek

ϵ	=	relative roughness, $\equiv \sigma/a$
ρ	=	fluid density, kg/m^3
μ	=	fluid viscosity, $kg/m.s$
σ	=	roughness standard deviation, m
ΔP	=	pressure gradient, Pa

Subscripts

0	=	reference value, smooth microtube
θ	=	in angular direction
x	=	in longitudinal direction

1 INTRODUCTION

Advances in fabrication methods in MEMS have generated significant interest in the area of microscale heat transfer and fluid flow. Microchannel heat exchangers can dissipate high heat fluxes which make them well-suited for a wide variety of unique cooling applications [1]. Microchannels can be integrated directly within the heat generating component; thus the thermal contact resistance at the interface of a heat-generating component and heat sink is eliminated. This feature leads to lower substrate temperatures and smaller temperature gradients that makes microchannels attractive for microelectronics cooling applications [2]. Microchannels are also used in other applications such as reactant delivery [3], physical particle separation [4], and inkjet print heads [5].

According to Obot [6], microchannels can be defined as tubes/channels whose diameters are less than 1 mm. There are many techniques used to manufacture microchannels, but the following four processes are more common [7]: i) Micromechanical machining e.g. diamond machin-

[1]Post-Doctoral Fellow. Mem. ASME. Corresponding author. E-mail: majid@mhtlab.uwaterloo.ca.
[2]Distinguished Professor Emeritus. Fellow ASME.
[3]Associate Professor and Director of MHTL. Mem. ASME.

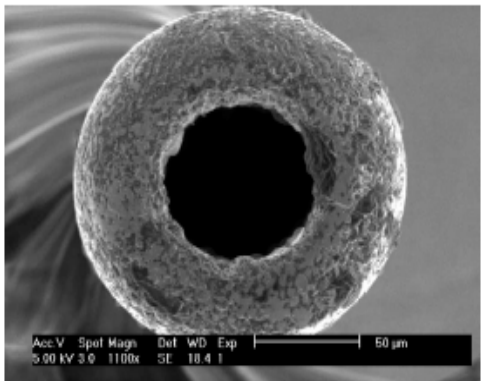

Figure 1. CROSS-SECTION OF A ROUGH MICROTUBE, FROM REF. [20]

ing, laser processes, microdrilling; ii) X-ray machining (such as LIGA LItographie-Galvanoforming-Abformung, iii) Photolithographic-based such as Si chemical etching, and iv) surface and surface-proximity-micromachining.

Many researchers have conducted experiments and reported friction factors higher than values predicted by conventional theory (smooth pipes) for liquids in microchannels during the last 15 years; see survey articles [2; 7; 8; 9]. Tuckerman [10] was the first to experimentally investigate the liquid flow and heat transfer in microchannels. He reported that the flow approximately followed the Hagen-Poiseuille theory. Pfahler et al. [11] and [12] conducted experimental studies on the fluid flow in microchannels. They observed that in the relatively large channels the experimental observations were in general agreement with the predictions from conventional equations. However, in the smallest of the channels, they observed a significant deviation from the classical predictions. Mala and Li [13] measured the friction factor of water in microtubes with diameters ranging from 50 to 254 μm. They also reported good agreements with the classical theory in large diameters microtubes. They proposed a roughness-viscosity model to explain the increase in the friction factor of the microchannels. The model of [13], however, did not encompass the physical mechanism and the effect of wall roughness. Li et al. [14] experimentally studied the frictional resistance for deionized water flow in microtubes. They reported a 15%-37% higher friction factor than the classical theory for rough microtubes. They concluded that the effect of wall roughness cannot be neglected for microtubes. However, they did not propose any model to explain the higher friction factors.

As the diameter of (micro-) tubes decreases the surface to volume ratio, which is equal to $2/r$, increases rapidly. As a result, the surface phenomena- including the effect of wall roughness, see Fig. 1, become more significant. There is a need for a better understanding of the effect of wall roughness on fluid characteristics in microtubes. No physical model exists in the literature that accounts for the wall roughness effects. This paper is the first attempt to develop a model to predict the pressure drop of the fully-developed laminar liquid flows in rough microtubes.

2 FRICTIONAL RESISTANCE

The flow regime through microtubes depends strongly on the method used to induce the motion of the fluid. The flow can be obtained in two ways: i) apply an external pressure gradient, i.e. *pressure driven* motion. In this case a Hagen-Poiseuille flow profile is generated along the channel. The Reynolds number associated with the flow is in general small, due to the small radii, the flow is usually laminar and the velocity varies across the entire cross-sectional area of the channel. ii) Apply an external electric field, i.e. *electrokinetically driven* flow. In this case the fluid velocity only varies within the so-called Debye screening layer near the channel walls. It is experimentally demonstrated that, in this case, the profile is practically uniform (slug flow) across the entire cross-section [15]. The focus of this study is on the pressure driven flow only.

In laminar flow at a sufficiently large distance from the entrance, the velocity distribution across the cross-section becomes independent of the coordinate along the direction of flow. The fluid moves under the influence of the pressure gradient which acts in the direction of the axis. Owing to friction, individual layers act on each other with shearing stress which is proportional to the velocity gradient in the axis normal to the direction of flow. Hence, a fluid flow particle is accelerated by the pressure gradient and retarded by the frictional shearing stress, i.e. no inertia forces exist. This flow is called Hagen-Poisuille.

Applying a force balance and the no-slip boundary condition, one can find a relationship between the mass flow rate $\dot{m}$ and the pressure gradient ΔP for a smooth circular tube of radius, a, as follows:

$$\dot{m} = \frac{\pi a^4}{8} \frac{\rho \Delta P}{\mu L} \tag{1}$$

where L, ρ, and μ are the length of the pipe ($L \gg a$), density, and viscosity of the fluid, respectively. Equation (1) states that the mass flow rate of the fluid is proportional to the pressure drop per unit length ($\Delta P/L$) and the fourth power of the pipe radius a. The mean velocity of the fluid is, $\overline{u} = \dot{m}/\pi\rho a^2$; thus the relation between the pressure gradient and the mean velocity is

$$\frac{\Delta P}{L} = \frac{8\mu\, \overline{u}}{a^2} \tag{2}$$

According to Darcy's formula, the friction factor, f, is defined by

$$f = \frac{\Delta P}{L}\frac{4a}{\rho\ \overline{u}^2} \tag{3}$$

It can easily be shown that $f = 64/Re_D$, where Re_D is the Reynolds number of a tube with a diameter $D = 2a$.

With the electrical network analogy in mind, we introduce a frictional resistance as:

$$\dot{m} = \frac{\Delta P}{R_{f,0}} \tag{4}$$

where $R_{f,0}$ is the frictional resistance of a smooth microtube of radius a and length L. Combining Eqs. (1) and (4), one finds

$$R_{f,0} = \frac{8\mu\ L}{\pi\rho\ a^4} \tag{5}$$

Note that the frictional resistance is not linearly proportional to the radius.

The relationship between the frictional resistance, defined in this study, and the Darcy's friction factor f is

$$f = \frac{4\pi\ a^3}{\overline{u}\ L}R_{f,0} \tag{6}$$

The concept of frictional resistance, introduced in Eq. (4), may also be used to construct frictional resistance networks to analyze more complex systems.

3 WALL ROUGHNESS

Roughness or surface texture can be thought of as the surface deviation from the nominal topography. The term *Gaussian* is used to describe a surface where its asperities are isotropic and randomly distributed over the surface. It is not easy to produce a wholly isotropic roughness.

According to Liu et al. [16] five types of instruments are currently available for measuring the surface topography: i) stylus-type surface profilometer, ii) optical (white-light interference) measurements, iii) Scanning Electron Microscope (SEM), iv) Atomic Force Microscope (AFM), and v) Scanning Tunneling Microscope (STM). Among these, the first two instruments are usually used for macro-to-macro asperity measurements, whereas the others may be used for micro or nanometric measurements. Surface texture is most commonly measured by a profilometer, which draws a stylus over a sample length of the surface. A datum or centerline is established by finding the straight line, or circular arc in the case of round components, from which the mean square deviation is a minimum. The arithmetic average of the absolute values of the measured profile height deviations, R_a, taken within a sampling length from the graphical centerline [17]. The value of R_a is

$$R_a = \frac{1}{l}\int_0^l |z\,(x)|\,dx \tag{7}$$

where l is the sampling length in the x direction and z is the measured value of the surface heights along this length. When the surface is Gaussian, the standard deviation σ is identical to the RMS value [18], R_q.

$$\sigma = R_q = \sqrt{\frac{1}{l}\int_0^l z^2\,(x)\,dx} \tag{8}$$

For a Gaussian surface, Ling [19] showed that the average and RMS values are related as follows:

$$R_q \approx \sqrt{\frac{\pi}{2}}R_a \approx 1.25R_a \tag{9}$$

4 FRICTIONAL RESISTANCE OF ROUGH MICROTUBES

The assumptions of the present model can be summarized as:

- the fully-developed laminar flow is modeled. The fluid is forced to move by a pressure gradient applied to the ends of the microtubes, i.e. pressure-driven flow.
- the fluid is Newtonian and the microtube cross-section is circular.
- the microtube walls are rough; the roughness is assumed to be Gaussian, i.e., isotropic in all directions. Also, there are no *macro* deviations or *waviness* inside the microtubes.
- rarefaction, compressibility, and slip-on-walls effects are negligible.
- fluid properties are constant.

Some researchers have reported that the transition from laminar to turbulent flow regimes starts at lower Reynolds numbers in microchannels. However, this early transition has not been observed by Judy et al. [20]. Also Obot [6] presented a critical review of published data and concluded that there is hardly any evidence to support the occurrence of transition of turbulence in smooth microchannels for Re < 1000. Therefore, the focus of this study is on the laminar flow regime and the transition will not be discussed.

Consider a long rough microtube with the mean radius of, a, and length $L \gg a$, Fig. 2. As shown schematically in the figure, the wall roughness of the microtube is assumed to posses a Gaussian distribution in the angular direction. Owing to the random nature of the wall roughness, an exact value of the local radius, r, can not be used for rough microtubes. Instead, probabilities of occurring different radii

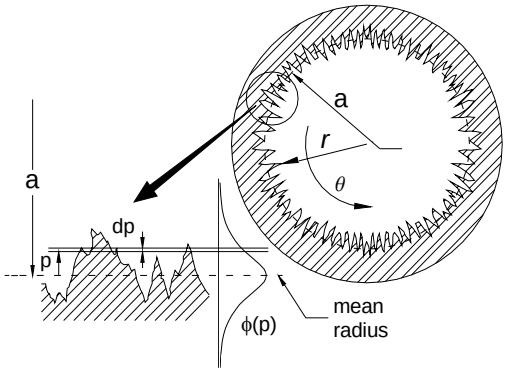

Figure 2. CROSS-SECTION OF A MICROTUBE: WALL ROUGHNESS AND GAUSSIAN DISTRIBUTION

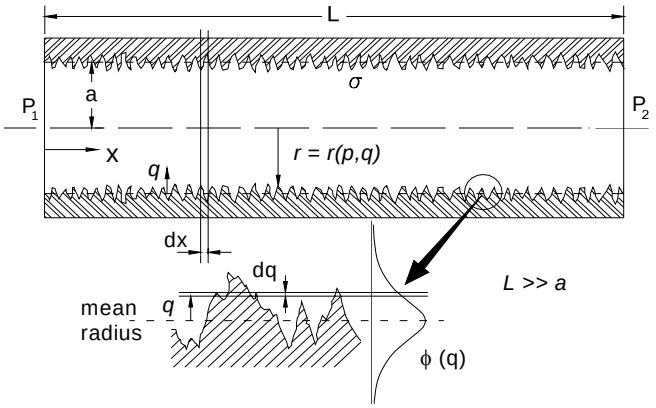

Figure 3. LONGITUDINAL CROSS-SECTION OF RANDOM ROUGH MICROTUBE

should be computed. A random variable, p, is used to represent the deviations of the local radius, r, in the angular direction, Fig. 2. The standard deviation of p is the wall roughness σ_θ and has the following Gaussian distribution:

$$\phi\left(p\right) = \frac{1}{\sqrt{2\pi}\sigma_\theta}\exp\left(-\frac{p^2}{2\ \sigma_\theta^2}\right) \tag{10}$$

The local radius can vary over a wide range of values from much larger to much smaller radii than the mean radius a, valleys and hills in the figure, with the Gaussian probability distribution shown in Eq. (10). The microtube wall also has roughness in the longitudinal direction x, see Fig. 3. The variations of the local radius of the microtube, r, in the longitudinal direction is shown by another random variable q, with the same Gaussian distribution as in the angular direction.

$$\phi\left(q\right) = \frac{1}{\sqrt{2\pi}\sigma_x}\exp\left(-\frac{q^2}{2\ \sigma_x^2}\right) \tag{11}$$

The local radius of the microtube can be written as

$$r = a + p + q \tag{12}$$

where a is the mean statistical value of the local radius, r, over the cross-sections over the entire length, L, of the microtube.

To better understand Eq. (12), consider cross-sections of a rough microtube at different longitudinal locations, Fig. 3. These cross-sections have different mean radii where the probability of these radii occurring can be determined from Eq. (11), $a+q$. Meanwhile, the actual radius at each cross-section varies around the mean radius, $a+q$, in the angular direction (variations of p) with the probability distribution described in Eq. (10). Therefore, the local radius of a microtube, r, is a function of both random variables p and q, i.e. $r = r(p,q)$. We assume that the local radius is the superposition of the two random variables, as shown in Eq. (12). Note that the variables p and q are independent. For argument sake, consider an imaginary case where a microtube has roughness only in the angular direction; thus one can write, $r = r(p)$. As a result, an average of these variables $[r = a + (p+q)/2]$ is not correct.

In the general case, the standard deviations σ_θ and σ_x might be different; however in this study, we assume an isotropic roughness, i.e. $\sigma_\theta = \sigma_x = \sigma$.

The frictional resistance dR_f for an infinitesimal element dx can be written using Eq. (5) as:

$$dR_f = \frac{8\mu\ dx}{\pi\rho}\int_{-\infty}^{+\infty}\int_{-\infty}^{+\infty}\frac{\phi\left(p\right)\ \phi\left(q\right)}{r^4}dp\ dq \tag{13}$$

Equation (13) considers the probabilities of all values of radius, r, occurring according to the Gaussian distribution. It also takes into account their effects on the frictional resistance dR_f. It should be noted that it is mathematically possible for the variables p and q to have values ranging from $-\infty$ to $+\infty$, see Eqs. (10) and (11). However, the probability of occurring much larger/ smaller radii than the mean radius, a, are quite small, see Fig. 6.

The total frictional resistance over the length, L, is

$$R_f = \frac{4\mu}{\pi^2\rho\sigma^2}\int_0^L\int_{-\infty}^{+\infty}\int_{-\infty}^{+\infty}\frac{\phi\left(p\right)\ \phi\left(q\right)}{\left(a+p+q\right)^4}dp\ dq\ dx \tag{14}$$

Equation (14) calculates an *effective* frictional resistance for rough microtubes. Integrating over the length L, one finds

$$R_f = \underbrace{\frac{8\mu L}{\pi\rho a^4}}_{R_{f,0}}\underbrace{\left\{\frac{1}{2\pi\sigma^2}\int_{-\infty}^{+\infty}\int_{-\infty}^{+\infty}\frac{\phi\left(p\right)\ \phi\left(q\right)}{\left(1+p/a+q/a\right)^4}dp\ dq\right\}}_{\text{effect of wall roughness on frictional resistance}} \tag{15}$$

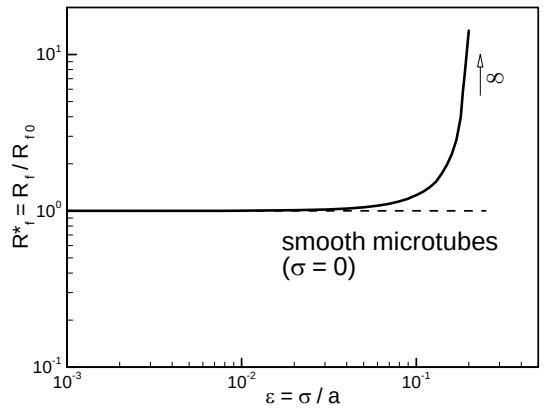

Figure 4. EFFECT OF WALL ROUGHNESS ON FRICTIONAL RESISTANCE

where $R_{f,0}$ is the frictional resistance of the smooth microtube, where no roughness exists, see Eq. (5). Thus, the effect of wall roughness on the frictional resistance can be presented as a normalized frictional resistance or a correction factor, i.e. $R_f^* = R_f/R_{f0}$. After changing variables and simplifying, one finds

$$R_f^* = \frac{1}{2\pi}\int_{-\infty}^{+\infty}\int_{-\infty}^{+\infty}\frac{\exp\left(-u^2/2\right)\ \exp\left(-v^2/2\right)}{\left[1+\epsilon\left(u+v\right)\right]^4}du\ dv \tag{16}$$

where ϵ is the relative wall roughness

$$\epsilon = \frac{\sigma}{a} \tag{17}$$

Note that in this study, the relative roughness, ϵ, is defined as the RMS wall roughness over the *radius* of the microtube. Whereas the conventional relative roughness is defined as roughness over *diameter*.

The integral in Eq. (16) can not be solved analytically; thus it must be solved numerically over a range of relative roughness. It can be shown that $\left[1+\epsilon\left(u+v\right)\right]^4 \cong \left(1+\epsilon u\right)^4\left(1+\epsilon v\right)^4$ where $\epsilon \ll 1$; thus Eq. (16) can be simplified to

$$R_f^* = \frac{1}{2\pi}\left\{\int_{-\infty}^{+\infty}\frac{\exp\left(-u^2/2\right)}{\left[1+\epsilon u\right]^4}du\right\}^2 \qquad \epsilon \ll 1 \tag{18}$$

The numerical solution to Eq. (16) is curve-fitted and the following correlations can be used to calculate R_f^*

$$R_f^* = \begin{cases} \dfrac{1}{1-23\ \epsilon^2} & \epsilon \leq 0.1 \\ \dfrac{1}{1-50\ \epsilon^{2.4}} & 0.1 < \ \epsilon < 0.15 \end{cases} \tag{19}$$

Table 1. EFFECT OF WALL ROUGHNESS ON FRICTIONAL RESISTANCE

relative roughness $\epsilon = \sigma/a$	normalized frictional resistance R_f^*
0.01	1.002
0.03	1.021
0.05	1.053
0.07	1.130
0.08	1.170
0.10	1.300
0.12	1.450

The accuracy of the above correlation is within a few percent of the numerical solution, less than 3%. Note that in the limit where roughness goes to zero, the effective frictional resistance predicted by the present model approaches the Hagen-Poisuille theory.

Figure 4 illustrates the trend of the normalized frictional resistance R_f^* as relative roughness ϵ is varied. Some values of R_f^* are listed in Table 1 to better demonstrate the effect of roughness on the pressure drop.

From Eq. (6), it can be shown that the effect of wall roughness on the friction factor f is the same as the frictional resistance, i.e.

$$f^* = \frac{f}{f_0} = R_f^* \tag{20}$$

Equations (20) and (19) can be employed to calculate the Darcy's friction factor for rough microtubes.

As shown in Fig. 4 and Table 1, the effect of roughness is negligible for relative roughness values $\epsilon < 0.03$. However, as relative roughness increases the correction factor R_f^* increases rapidly, e.g. for a microtube with a relative roughness of 0.08, an increase of ≈17% in frictional resistance is predicted by the present model. As ϵ increases to approximately ≈0.2, the normalized frictional resistance approaches infinity.

It should be noted that the relative roughness of 0.2 is extremely high, imagine a microtube where its wall roughness (standard deviation) is 1/5 of its radius. It is also worth noting that in the Gaussian distribution as the standard deviation increases, the probability of occurring radii with larger deviations from the mean radius becomes higher, see Fig. 6. In other words, in rougher microtubes-higher values of σ- the probability of occurring smaller radii is higher, which leads to higher pressure drops.

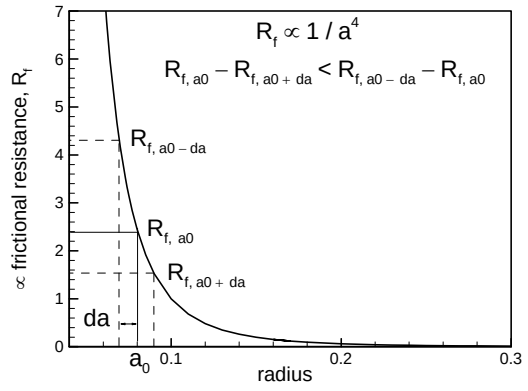

Figure 5. RELATIONSHIP BETWEEN FRICTIONAL RESISTANCE AND RADIUS OF ROUGH MICROTUBES

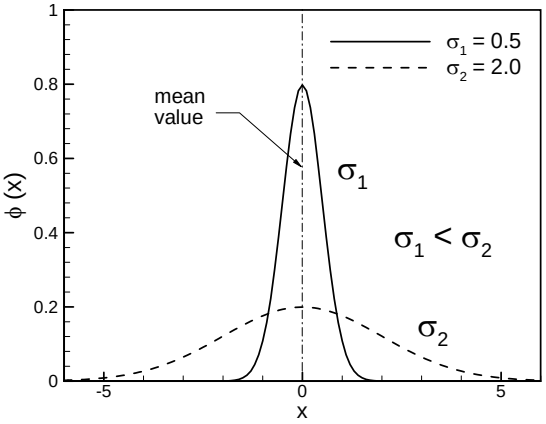

Figure 6. GAUSSIAN DISTRIBUTION

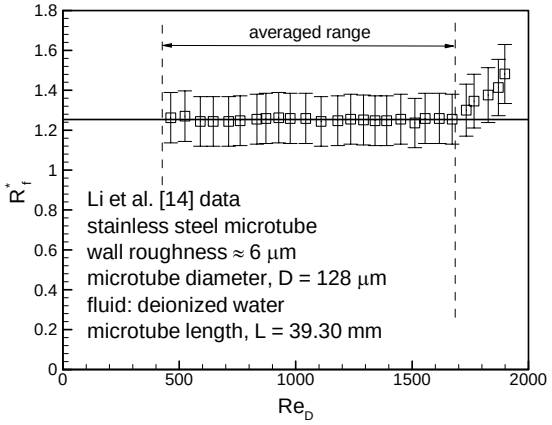

Figure 7. COMPARISON OF PRESENT MODEL TO LI ET AL. [14] DATA, $D = 128\ \mu m$

As seen in Fig. 4, increasing roughness, while all other parameters are kept constant, results in an increase in the frictional resistance or equivalently the pressure drop, see Eq. (20). We know that by assuming the Gaussian distribution, the probabilities of having smaller and/or larger radii microtubes (than the mean radius a) are identical; also the mean statistical radius of the microtube remains unchanged as the roughness is increased. Then the question may arise: why the frictional resistance increases as roughness increases? The answer to this question lies in the relationship between the frictional resistance and the radius of microtube, Eq. (5). The frictional resistance is inversely proportional to the radius to the fourth power, $R_f \propto 1/a^4$. Figure 5 illustrates the frictional resistance as a function of the radius. The frictional resistance of a slightly smaller radius $(a_0 - da)$ is much larger than the resistance of a slightly larger radius $(a_0 + da)$, see Fig. 5. Therefore, the resistance of smaller radii microtubes controls the effective frictional resistance, and that is why the frictional resistance increases as a microtube becomes rougher.

5 COMPARISON WITH DATA

In this section, the present model is compared to published data where the wall roughness was reported/measured.

Table 2 summarizes the experimental data that have been used in the comparison. A constant roughness value is used for the same microtube material for all radii reported in each reference. In other words, the roughness is assumed *not* to be a function of the microtube radius. This assumption may not be strictly correct, unfortunately none of the available experimental studies reported the wall roughness for different radii of microtubes. Different values for the uncertainty of the experimental data were reported by different researchers all in the vicinity of 10%; thus, a constant error bound of 10% is considered for all data.

Li et al. [14] used glass, silicon and stainless steel microtubes with diameters ranging from 79.9 to 166.3 μm, from 100.25 to 205.3 μm, and from 128.76 to 179.8 μm, respectively. To determine the wall conditions, the three types of microtubes were milled open along the axial direction. The wall roughness was measured using a Talysurf-120 profilometer. The wall roughness of glass and silicon microtubes were reported in order of 0.05 μm; thus the glass and the silicon microtubes can be considered as smooth microtubes. However, the stainless steel microtubes exhibited a relatively large wall roughness. They [14] did not report the exact value of R_q or R_a for wall roughness; only a "peak-

Table 2. SUMMARY OF EXPERIMENTAL DATA USED IN COMPARISON

Code	Reference	D (μm)	$\sigma \approx$ (μm)	Notes
CCGZ	Celata et al. [21]	130	4.31	microtube: AISI316 stainless steel, liquid: R-114 $100 < Re_D < 8000$ a statistical method used to measure R_a
JZHL	Jiang et al. [22]	$8 - 42$	0.3	microtube: silicon, liquid: deionized water $0.12 < Re_D < 3$ microscopic image snaps used to measure roughness
KSS	Kandlikar et al. [23]	1076	$2.4 - 3.73$	microtube: stainless steel, liquid: water $500 < Re_D < 2500$ Alpha-Step 200 profilometer used to measure R_a
LDG	Li et al. [14]	$128 - 179$	6	microtube: stainless steel, liquid: deionized water $500 < Re_D < 2500$ a Talysurf-120 profilometer used to measure roughness
ML	Mala and Li [13]	SST: $63 - 254$ FST: $50 - 250$	2.5 2.0	microtube: stainless steel (SST), fused silica (FST) $100 < Re_D < 2500$, liquid: deionized water manufacturer info reported for roughness, no measurements

valley roughness" in the order of ≈ 5.5 μm was reported for stainless steel microtubes. Through experiments, Li et al. showed that for glass and silicon microtubes the conventional theory in the laminar regime holds. For stainless steel microtubes the friction factors were higher than the prediction of the classical theory. Figures 7 to 9 show the comparison between the present model, Eq. (19), and some of the [14] data sets. As can be seen, the model shows good agreement with these data.

Mala and Li [13] studied experimentally the flow of deionized water through circular microtubes of fused silica and stainless steel with diameters ranging between 50 to 254 μm. They reported a strange non-linear trend between pressure drop and flow rate for low Reynolds numbers, and that the friction factors were consistently higher than the conventional values. Figures 10 and 11 represents the comparison between the model and two sets of the [13] data.

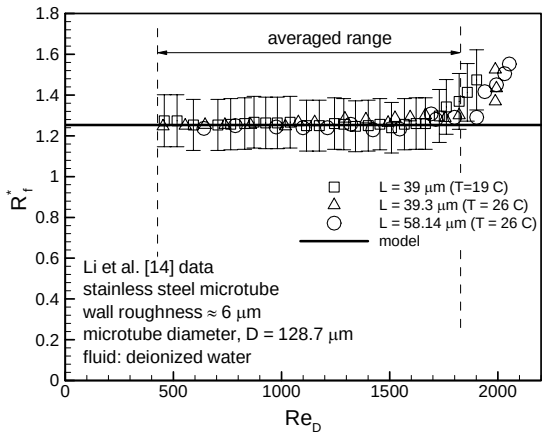

Figure 8. COMPARISON OF PRESENT MODEL TO LI ET AL. [14], $D = 128$ μm, $T = 19, 26^\circ C$

Jiang et al. [22] studied the trend of water flow through glass microtubes. Their circular microtubes were fabricated by the glass drawn process, with wall roughness in the order of 0.3 μm. The microtubes diameters ranged from 8 to 42 μm. The range of the Reynolds number, in which their experiments were conducted, was very low, see Table 2. However, they did not report any trends similar to those of Mala and Li [13]. Figure 12 shows the comparison

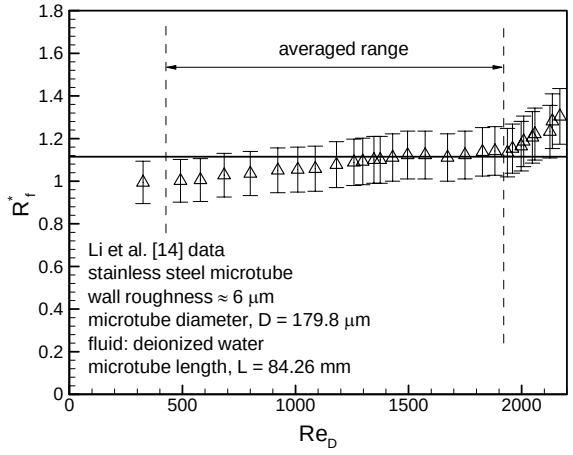

Figure 9. COMPARISON OF PRESENT MODEL TO LI ET AL. [14], $D = 179\ \mu m$

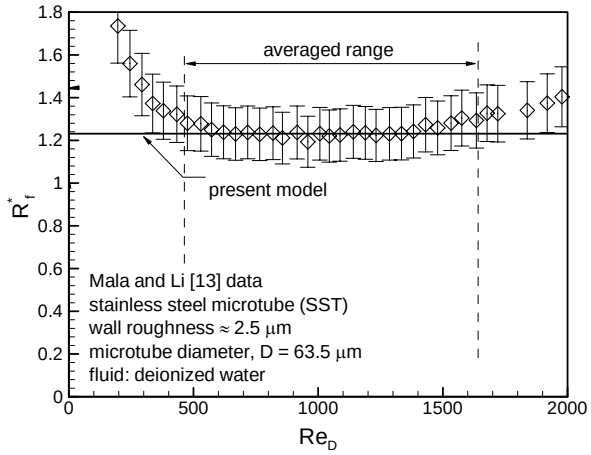

Figure 10. COMPARISON OF PRESENT MODEL TO MALA AND LI. [13], STAINLESS STEEL, $D = 63.5\ \mu m$

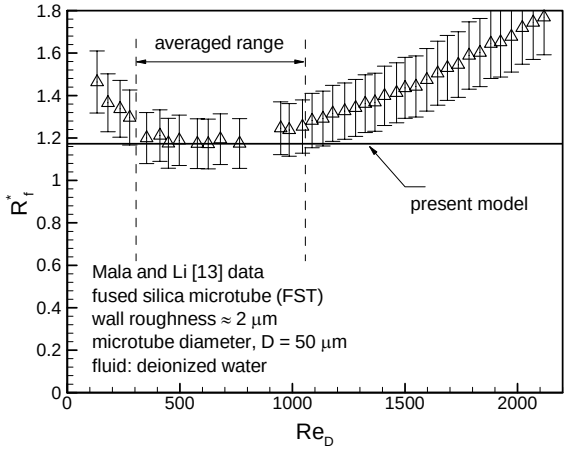

Figure 11. COMPARISON OF PRESENT MODEL TO MALA AND LI. [13], FUSED SILICA, $D = 50\ \mu m$

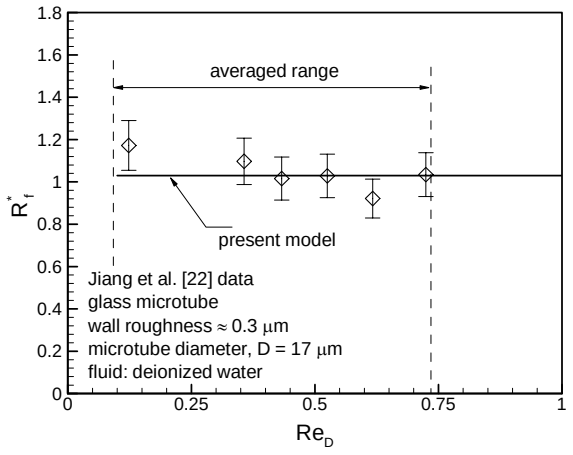

Figure 12. COMPARISON OF PRESENT MODEL TO JIANG ET AL. [22], GLASS, $D = 17\ \mu m$

between the present model and a set of the [22] data.

Celata et al. [21] performed an experimental analysis of the friction factor in stainless steel capillary tubes with a diameter of 130 μm with R114 as the fluid, see Table 2. Their reported values of R_a have been converted to $\sigma = R_q$, using Eq. (9), to be used in the comparison.

Kandlikar et al. [23] investigated experimentally the role of the wall roughness on the pressure drop in two microtubes with different diameters 1067 and 620 μm. The wall roughness of microtube walls was changed by etching with an acid solution. A micrograph scan of the microtubes was used to measure the average roughness, R_a, see Eq. (7). Their reported values of R_a have been converted to $\sigma = R_q$, using Eq. (9), to be used in the comparison.

The frictional resistance constant, $C = fRe_D$, is not a function of Reynolds number and remains unchanged for the laminar regime. Therefore, the experimental data are averaged over the laminar region; the transitional data are *not* included in the comparison. For each data set, the relative roughness is calculated using $\epsilon = \sigma/a$. As a result, for each experiment data set, a relative roughness and a normalized frictional resistance can be obtained, dashed lines in Figs. 7 to 12 demarcate the averaged ranges. Figure 13 shows the experimental normalized frictional resistance as a function of their relative roughness; for assigned codes to experimental data sets see Table 2. As previously men-

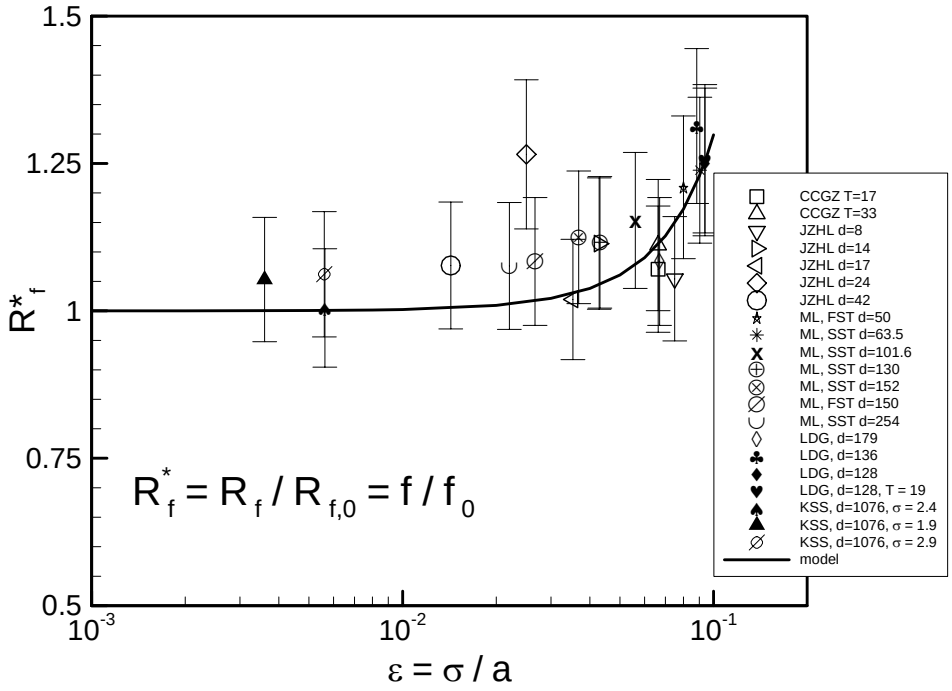

Figure 13. EFFECT OF RELATIVE ROUGHNESS ON PRESSURE DROP OF MICROTUBES: COMPARISON OF PRESENT MODEL WITH ALL DATA

tioned, the non-linear trend of Mala and Li [13] data (at low Re numbers) has not been observed by any other researchers. Therefore, those data points are not included in the averaged values shown in Fig. 13. The agreement between the model and the data is relatively good; within the 10% for most of data points. More importantly, the present model shows the trends of the data as relative roughness increases.

6 SUMMARY AND CONCLUSIONS

The influence of wall roughness on the laminar, fully developed liquid flow in microtubes is studied and a new model is proposed. The concept of frictional resistance is introduced and its relation to the Darcy's friction coefficient is derived.

The present model assumes an isotropic Gaussian distribution for wall roughness. Also, the rarefaction, compressibility, and slip-on-wall effects are assumed to be negligible. Owing to the random nature of the wall roughness, an exact value of the local radius can not be used for rough microtubes. Instead, probabilities of occurring different radii should be computed. Two independent random variables are considered to account for the deviations of the local radius in the angular and longitudinal directions. The local radius of a microtube is a function of these two random variables. In the present model, the local radius is assumed to be the superposition of the two random variables. The effect of wall roughness on the frictional resistance is presented as a normalized frictional resistance or a correction factor; the final results are reported in the form of a compact correlation. It is found that the effect of roughness is to increase the pressure drop in microtubes. The effect of roughness can be neglected when relative roughness is less than 3%. It is observed that the constant in the conventional frictional resistance, $C = fRe_D$, is a function of relative roughness, i.e. $C = C(\epsilon)$. The published experimental data, in which the roughness is reported, are collected and compared with the present model. The present model exhibits the influence of roughness and predicts the pressure drop within the uncertainty of data.

There is a need for carefully designed experimentation aimed at more comprehensive wall roughness and pressure drop measurements. For most conventional microtubes, the relative roughness is small, in the order of few percent. According to the model, the increase in the pressure drop for these microtubes are within the uncertainty of the current experimental arrangements, i.e. 10%. This makes the validation of the present model for relatively smooth microtube a difficult task.

ACKNOWLEDGMENT

The authors gratefully acknowledge the financial support of the Centre for Microelectronics Assembly and Packaging, CMAP and the Natural Sciences and Engineering Research Council of Canada, NSERC. Our thanks go to Mr. K. Narimani for his helpful comments on Section 4.

REFERENCES

[1] D. B. Tuckerman and R. F. Pease, "High-performance heat sinking for vlsi," *IEEE Electronic Device Letters*, no. 5, pp. 126–129, 1981.

[2] C. B. Sobhan and S. V. Garimella, "A comparative analysis of studies on heat transfer and fluid flow in microchannels," *Microscale Thermophysical Engineering*, vol. 5, no. 4, pp. 293–311, 2001.

[3] A. V. D. Berg, W. Olthius, and P. Bergveld, *Micro Total Analysis Systems*. Boston, MA, U.S.A: Kluwer Academic Press, 2000.

[4] R. Reston and E. Kolesar, "Silicon-miromachined gas chromatography system used to separate and detect ammonia and nitrogen dioxide," *Journal of Microelectromechanical Systems*, vol. 65, pp. 2637–2642, 1994.

[5] R. Allen, J. Meyer, and W. Knight, "Thermodynamics and hydrodynamics of thermal ink jets," *Hewlett-Packard Journal*, vol. 36, no. 5, pp. 21–27, 1985.

[6] N. T. Obot, "Toward a better understanding of friction and heat/mass transfer in microchannels- a literature review," *Microscale Thermophysical Engineering*, vol. 6, pp. 155–173, 2002.

[7] G. L. Morini, "Single-phase convective heat transfer in microchannels: A review of experimental results," *International Journal of Thermal Sciences*, vol. 43, pp. 631–651, 2004.

[8] A. B. Duncan and G. P. Peterson, "Review of microscale heat transfer," *Journal of Applied Mechanics Review*, vol. 47, pp. 397–428, 1994.

[9] I. Papautsky and T. Ameel, "A review of laminar single-phase flow in microchannels," *ASME, Proceedings of Int. Mech. Eng Congress Expos Proc (IMECE) 2001, ASME, New York*, vol. 2, pp. 3067–3075, 2001.

[10] D. B. Tuckerman, *Heat Transfer Microstructures for Integrated Circuits*. PhD thesis, Stanford University, Dept. of Electrical Eng., California, USA, 1984.

[11] J. Pfahler, J. Harley, H. H. Bau, and J. Zemel, "Liquid and gas transport in small channels," *ASME Dynamic Systems and Control Division (Publication) DSC, Microstructures, Sensors, and Actuators*, vol. 19, pp. 149–157, 1990.

[12] J. Pfahler, J. Harley, and H. H. Zemel, "Gas and liquid flow in small channels," *ASME Dynamic Systems and Control Division (Publication) DSC, Microstructures, Sensors, and Actuators*, vol. 32, pp. 49–60, 1991.

[13] G. M. Mala and D. Q. Li, "Flow characteristics of water in microtubes," *International Journal of Heat Fluid Flow*, vol. 20, no. 2, pp. 142–148, 1999.

[14] Z. Li, D. Du, and Z. Guo, "Experimental study on flow characteristics of liquid in circular microtubes," *Microscale Thermophysical Engineering*, vol. 7, no. 3, pp. 253–265, 2003.

[15] G. M. Whitesides and A. D. Stroock, "Flexible methods for microfluidics," *Physics Today*, vol. 6, pp. 42–48, 2001.

[16] G. Liu, Q. Wang, and C. Ling, "A survey of current models for simulating contact between rough surfaces," *Tribology Trans.*, vol. 42, no. 3, pp. 581–591, 1999.

[17] "Ansi b46.1: Surface texture: Surface roughness, waviness and lay," 1985.

[18] K. L. Johnson, *Contact Mechanics*, ch. 13. Cambridge, UK: Cambridge University Press, 1985.

[19] F. F. Ling, "On asperity distributions of metalic surfaces," *Journal of Applied Physics*, vol. 29, no. 8, 1958.

[20] J. Judy, D. Maynes, and B. W. Webb, "Characterization of frictional pressure drop for liquid flows through microchannels," *International Journal of Heat and Mass Transfer*, vol. 45, pp. 3477–3489, 2002.

[21] G. Celata, M. Cumo, M. Guglielmi, and G. Zummo, "Experimental investigation of hydraulic and single phase heat transfer in 0.130 mm capillary tube," *Eng. 6, Microscale Thermophys*, pp. 85–97, 2002.

[22] X. N. Jiang, X. Y. Huang, and C. Y. Liu, "Laminar flow through microchannels used for microscale cooling systems," *IEEE CPMT Electronic Packaging Technology Conference*, pp. 119–122, 1997.

[23] S. G. Kandlikar, S. Joshi, and S. Tian, "Effect of channel roughness on heat transfer and fluid flow characteristics at low reynolds numbers in small diameter tubes," *Proceedings of the National Heat Transfer Conference, ASME*, vol. 2, pp. 1609–1618, 2001.